FORMATION OF PERIODICAL MAGNETIC FIELDS BY SEQUENCE OF RINGS WITH DIFFERENT ELECTRIC AND MAGNETIC PROPERTIES

D.Yu. Kopiychenko, I.N. Onishchenko, G.V. Sotnikov, S.S. Pushkarev, Yu.V. Prokopenko, P.T. Chupikov, D.V. Medvedev
NSC "Kharkov Institute of Physics and Technology"
Akademicheskaya 1, 61108, Kharkov, Ukraine;
phone: (0572)356623;
E-mail: sotnikov@kipt.kharkov.ua

The electrodynamics analysis of topography of magnetic fields originating in spatially periodic system is carried out. The system under investigation is the solenoid inside which rings made from materials differ in electric and magnetic properties are periodically placed. The system of equations connecting amplitudes of spatial harmonics of the field is obtained. This system is parsed numerically. Requirements are determined when in the spatial structure of a magnetic field the dominating role is played by the main harmonic. The amplitudes of longitudinal and transverse components of the modulated magnetic field as a function of the ring sizes, current frequency, magnetic and electric properties of rings materials are investigated. The amplitudes of the fields obtained in the full electrodynamics consideration are compared with the amplitudes of a periodic magnetic field, obtained in an impedance approximation.

PACS: 41.85.Lc

I. INTRODUCTION

Spatially periodic media are widely applied as slowing down structures in the accelerating technique [1,2], in the high-current electron beams focusing schemes [3], in powerful UHF electron devices [4]. One of new applications of periodic magnetic media is the spatial modulation of an electronic beam in a collective ion accelerator [5]. For these purposes the rings from materials with different magnetic properties, located in the homogeneous magnetic field, can be used. Magnitude and modulation of the magnetic field, created by such a system, in practice is defined by experimental measuring results [6]. The theoretical analysis is restricted to impedance approximation [4] by the assignment of tangential value of magnetic induction at ring surfaces. In this case magnitude and modulation law of the magnetic field in drift chamber aren't interlinked neither to value of a magnetic field of the solenoid nor with magnetic and electrical properties of rings. In the present work exact electrodynamics calculation of a cylindrical wiggler on the basis of the solenoid loaded with rings having different magnetic properties is carried out

II. THE SET OF EQUATIONS

We shall conventionally divide the investigated volume into three areas in a cross-section: area I - the vacuum drift channel, area II - rings, III - exterior vacuum area. On the boundary of areas II and III the azimuth current slowly varying with frequency ω and creating in absence of rings the magnetic field with the strength amplitude equal to H_0 is given. For simplification of the analysis we shall neglect the thickness of solenoid walls. We shall divide area II into two parts: A and B, differing by values of permittivity and permeability.

The magnetic field originating in such a system, can be found by the method of partial areas when solving Maxwell equations for H - wave in each of the mentioned areas and matching the solutions at conjoint boundaries. The longitudinal component of the induction density vector B_z and transversal component of the magnetic intensity vector H_r in each of partial regions I, II and III are defined from the equations

$$\frac{1}{r}\frac{\partial}{\partial r}\left(r\frac{\partial B_z}{\partial r}\right)+\mu(z)\frac{\partial}{\partial z}\left(\frac{1}{\mu(z)}\frac{\partial B_z}{\partial z}\right)+k^2\varepsilon(z)\mu(z)B_z=0,$$

$$\frac{\mu(z)}{r}\frac{\partial}{\partial r}(rH_r)+\frac{\partial B_z}{\partial z}=0,$$

where: $k^2=\omega^2/c^2$. In the areas I and III $\varepsilon=1$, $\mu=1$ and in the IIA area $(0<z<a)$ $\varepsilon=\varepsilon_1$, $\mu=\mu_1$ and in the IIB area $(-b<z<0)$ $\varepsilon=\varepsilon_2$, $\mu=\mu_2$.

Due to the periodicity of the structure we shall search for solutions in the one period $L_w=a+b$. As equation (1) supposes variables separation we search for the solution in the form: $B_z=\sum_n R_n(r)\cdot Z_n(z)$. From (1) we have obtained the equations for the functions $R_n(r)$ and $Z_n(z)$:

$$\frac{1}{r}\frac{d}{dr}\left(r\frac{dR_n(r)}{dr}\right)+k_{rn}^2R_n(r)=0$$

$$\mu\frac{d}{dz}\left(\frac{1}{\mu}\frac{dZ_n(z)}{\partial z}\right)+k_{zn}^2Z_n(z)=0$$

where transverse k_r and longitudinal k_z wave numbers are connected with ratio $k_{zn}^2+k_{rn}^2=k^2\varepsilon\mu$.

In areas I and III we search for the solution as:

$$B_z^I=\sum_{n=-\infty}^{n=+\infty}C_{1n}J_0(\kappa_{rn}r)exp(ik_{zn}z),$$

$$B_z^{III}=\sum_{n=-\infty}^{n=+\infty}C_{3n}H_0^I(\kappa_{rn}r)exp(ik_{zn}z),$$

where $k_{zn} = 2\pi n/L + k_3$ satisfies Floque's relation and $\kappa_{rn} = \sqrt{k^2 - k_{zn}^2}$.

In the area II we shall search for solutions of set of equations by the separately in each of region constancy ε and μ in form traveling forward and backward waves:

$$B_z^{IIA} = \sum_{n=0}^{+\infty} \left(C_{2n} J_0(k_{rn} r) + D_{2n} N_0(k_{rn} r)\right) \left(A_{21}^n exp(ik_{1zn} z) + B_{21}^n exp(-ik_{1zn} z)\right),$$

$$B_z^{IIB} = \sum_{n=0}^{+\infty} \left(C_{2n} J_0(k_{rn} r) + D_{2n} N_0(k_{rn} r)\right) \left(A_{22}^n exp(ik_{2zn} z) + B_{22}^n exp(-ik_{2zn} z)\right),$$

where k_{rn} and respectively $k_{1zn} = \sqrt{k^2 \varepsilon_1 \mu_1 - k_{rn}^2}$ and $k_{2zn} = \sqrt{k^2 \varepsilon_2 \mu_2 - k_{rn}^2}$ are defined from the boundary conditions

$$B_z^{IIA}\Big|_{z=0} = B_z^{IIB}\Big|_{z=0}, \quad H_r^{IIA}\Big|_{z=0} = H_r^{IIB}\Big|_{z=0},$$

$$B_z^{IIA}\Big|_{z=a} = B_z^{IIB}\Big|_{z=a}, \quad H_r^{IIA}\Big|_{z=a} = H_r^{IIB}\Big|_{z=a}$$

and requirements of periodicity

$$B_z^{IIB}\Big|_{z=a} = B_z^{IIB}\Big|_{z=-b} \cdot exp(-ik_3 L),$$

$$H_r^{IIB}\Big|_{z=a} = H_r^{IIB}\Big|_{z=-b} \cdot exp(-ik_3 L).$$

Substituting (5) in boundary conditions (6) and (7) we obtain the characteristic equation

$$\cos k_3 L = \cos k_{1zn} a \cos k_{2zn} b - \frac{\left(k_{1zn}\mu_2\right)^2 + \left(k_{2zn}\mu_1\right)^2}{2k_{1zn}k_{2zn}\mu_1\mu_2} \sin k_{1zn} a \sin k_{2zn} b.$$

It is necessary to note, that the characteristic equation in the form (8) coincides with the equation received in [1] for waveguide, loaded with continuous dielectric disks. Essential difference of our case is that transverse wave number k_r is not the given, and should be defined itself from the solution of this equation. Thus we fix frequency of a wave.

Solving (8) with respect to k_{rn} we obtain two set of solutions k_{1rn} and k_{2rn}. The general solution quantity equals to $2N+1$, where $N = \max n$. Worth to note that getting equation (9) we turned down two solutions corresponded $k_{1zn} = 0$ and $k_{2zn} = 0$, because these solutions lead to zero values of the constants $A_{21}^n, B_{21}^n, A_{22}^n, B_{22}^n$. The general solution in the second area is defined as:

$$B_z^{IIA} = \sum_{n=-\infty}^{+\infty} \left(C_2^n J_0(k_{rn} r) + D_2^n N_0(k_{rn} r)\right) \left(exp(ik_{1zn} z) + F_{B1}(k_{1rn}) exp(-ik_{1zn} z)\right)$$

$$B_z^{IIB} = \sum_{n=-\infty}^{+\infty} \left(C_2^n J_0(k_{rn} r) + D_2^n N_0(k_{rn} r)\right) \left(F_{A2}(k_{rn}) exp(ik_{2zn} z) + F_{B2}(k_{rn}) exp(-ik_{2zn} z)\right),$$

where $F_{B1}(k_{rn}) = \frac{B_{21}^n}{A_{21}^n}$, $F_{A2}(k_{rn}) = \frac{A_{22}^n}{A_{21}^n}$, $F_{B2}(k_{rn}) = \frac{B_{22}^n}{A_{21}^n}$.

The constants figuring in solutions (4) and (8) are determined from the radial boundary conditions

$$H_z^I\Big|_{r=ra} = H_z^{II}\Big|_{r=ra}, \quad B_r^I\Big|_{r=ra} = B_r^{II}\Big|_{r=ra},$$

$$H_z^{II}\Big|_{r=rb} = H_z^{III}\Big|_{r=rb} + G, \quad B_r^{II}\Big|_{r=rb} = B_r^{III}\Big|_{r=rb}.$$

Having substituted (4), (5) in (11) we shall obtain the infinite system of the linear inhomogeneous equations concerning constants. Because of awkwardness we do not give it here. Having solved it and having done return substitutions, we shall obtain expressions for a magnetic field in each of partial regions.

III. ANALYTICAL SOLUTION OF THE CHARACTERISTIC EQUATION

In the practically important case, when $\mu_2/\mu_1 << 1$, characteristic equation (8) allows approximate analytical solution. In this case more convenient to solve this equation concerning k_{zn} instead of k_{rn}.

Looking for the first series solutions as $k_{1zn} = (\pi n + \delta_{1n})/a$, where $\delta_{1n} << 1$, we obtain

$$\delta_{1n} = -\frac{2\pi n k_{2zn}\left(\cos(k_3 L) - (-1)^n \cos(k_{2zn} b)\right)}{a\left(\left(\frac{\pi n}{a}\right)^2 \frac{\mu_2}{\mu_1} + \left(k_{2zn}\right)^2 \frac{\mu_1}{\mu_2}\right)\sin(k_{2zn} b)}, n > 0$$

$$\delta_{10} = \sqrt{\frac{2\left(\cos(k_3 L) - \cos(k_{2z0} b)\right)\frac{k_{2z0}}{a} + k_{2z0}^2 \frac{\mu_1}{\mu_2}\sin(k_{2z0} b)}{\frac{k_{2z0}}{a}\cos(k_{2z0} b) + \left(\frac{1}{a^2}\frac{\mu_2}{\mu_1} - \frac{1}{6}\frac{\mu_1}{\mu_2}k_{2z0}^2\right)\sin(k_{2z0} b)}},$$

where $k_{2zn} = \sqrt{k^2\left(\varepsilon_2\mu_2 - \varepsilon_1\mu_1\right) + \left(\frac{\pi n}{a}\right)^2}$.

Looking for the second series solutions as $k_{2zn} = \frac{\pi n + \delta_{2n}}{b}$, where $\delta_{2n} << 1$, we obtain

$$\delta_{2n} = -\frac{2\pi n k_{1zn}\left(\cos(k_3 L) - (-1)^n \cos(k_{1zn} a)\right)}{b\left(\left(\frac{\pi n}{b}\right)^2 \frac{\mu_1}{\mu_2} + \left(k_{1zn}\right)^2 \frac{\mu_2}{\mu_1}\right)\sin(k_{1zn} a)}, n > 0$$

$$\delta_{20} = \sqrt{\frac{2\left(\cos(k_3 L) - \cos(k_{1z0} a)\right)\frac{k_{1z0}}{b} + k_{1z0}^2 \frac{\mu_2}{\mu_1}\sin(k_{1z0} a)}{\frac{k_{1z0}}{b}\cos(k_{1z0} a) + \left(\frac{1}{b^2}\frac{\mu_1}{\mu_2} - \frac{1}{6}\frac{\mu_2}{\mu_1}k_{1z0}^2\right)\sin(k_{1z0} a)}},$$

where $k_{1zn} = \sqrt{k^2\left(\varepsilon_1\mu_1 - \varepsilon_2\mu_2\right) + \left(\frac{\pi n}{b}\right)^2}$.

At constant values concerning experimental installation parameters these expressions become notable simpler as $1 >> \delta_1 \geq \mu_2/\mu_1 >> k_3 L$,

$$\frac{\left|k\sqrt{\left(\varepsilon_1\mu_1 - \varepsilon_2\mu_2\right)}\right|}{\pi n/L} >> 1, n < 100:$$

$$\delta_{1n} = 2i(-1)^n \alpha\left(k_{1zn}\right) + o\left(\frac{\mu_2}{\mu_1}\right), n > 0$$

$$\delta_{2n} = 2i(-1)^{n+1}\alpha(k_{1zn}) + o\left(\frac{\mu_2}{\mu_1}\right), n > 0$$

$$\delta_{20} = \sqrt{-2ik_{1zn}b\frac{\mu_2}{\mu_1} + o\left(\frac{\mu_2}{\mu_1}\right)},$$

where $\alpha(k_{1zn}) = k_{1zn}\mu_2 / k_{2zn}\mu_1$.

It is easily seen that equation (9) has no solution close to $k_{1zn} = 0$.

When $k_{1zn} = (\pi n + \delta_{1n})/a$, and $\left|k\sqrt{(\varepsilon_1\mu_1 - \varepsilon_2\mu_2)}\right| >> \pi n/L$, $n < 100$ (this means $\mathrm{Im}(k_{1zn}b) << -1$)) correlations between constants become lot simpler too by decomposition on $e^{\mathrm{Im}(k_{2zn}b)}$:

$$F_{B1}(k_{rn}) = -\frac{1-\alpha(k_{1zn})}{1+\alpha(k_{1zn})} + o(1),$$

$$F_{A2}(k_{rn}) = \frac{2\alpha(k_{1zn})}{1+\alpha(k_{1zn})} + o(1),$$

$$F_{B2}(k_{rn}) = \frac{2(-1)^n(\alpha(k_{1zn}) + i\delta_{1n})}{1+\alpha(k_{1zn})}e^{\mathrm{Im}(k_{2zn}b)} + o\left(e^{\mathrm{Im}(k_{2zn}b)}\right).$$

It is seen that only $F_{B2}(k_{rn})$ essentially depends on δ_{1n} (as $\alpha(k_{1zn})$ weakly changes with changing of δ_{1n}).

IV. NUMERICAL CALCULATIONS

We carried out numerical calculations for parameters of experimental installation "Agate" [7] in two variants with iron and aluminum rings and only with iron rings: $a = 2cm$, $b = 2cm$, $R_1 = 2.5cm$, $R_2 = 3,3cm$, $H_0 = 1kOe$, $\mu_1 = 5000$, $\mu_2 = 1$, $\sigma_1 = 1,05\cdot10^{17}s^{-1}$, $\sigma_2 = 3,60\cdot10^{17}s^{-1}$, $\varepsilon_{1,2} = 1 + 4\pi i\sigma_{1,2}/\omega$, $\omega = \frac{2\pi}{\tau}$, $\tau = 15ms$, $k_3 = 100k$. In the case of only iron rings $\varepsilon_2 = 1$. In the next analysis's we shall take these parameters for the base and shall investigate the changing of magnetic induction as variation of one of these.

In Fig.1 and Fig.2 the two-dimensional structures of the magnetic field created by a periodic system of iron and aluminum rings and of iron rings and vacuum (in this case $\sigma_2 = 0$) are shown. The quantitative pattern of the magnetic field topography corresponds to the qualitative ideas about the magnetic field behavior depending on a selected view point that confirms correctness of the carried out analytical and numerical calculations.

The infinite sums in the field expressions were substituted for finite sums ($-N \le n \le N$) in calculations.

In Fig.3 the longitudinal topography of axial component of the magnetic induction vector on the axis of the system and on the radius $r = 1.6cm$ for both variants are shown. As results from graphs, apart $1,6\ cm$ from the waveguide axis (at the surface of the thin electron beam which is going into the second section of the accelerating installation "Agate" [7]) the depth of modulation is about 56%.

The base contribution to magnetic field modulation is given with a harmonic $n = 1$. On the axis of the system the modulation depth is about 33%.

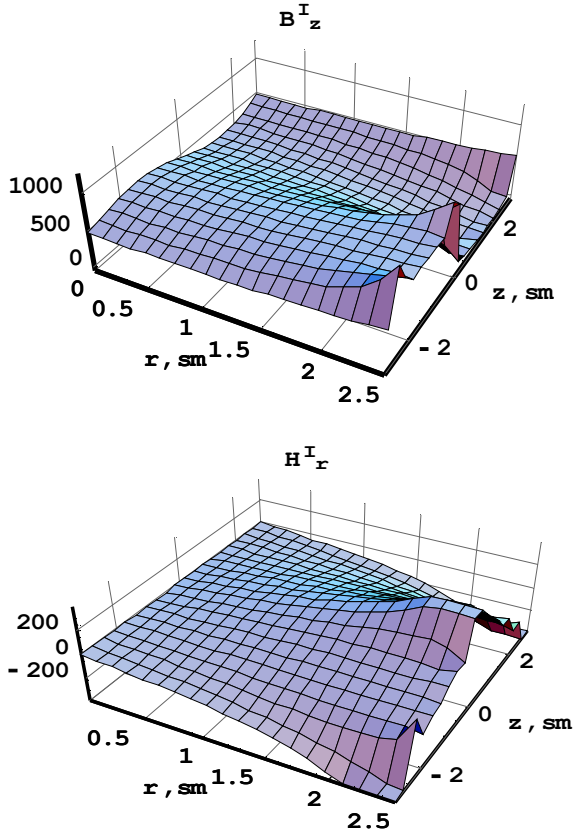

Fig.1. Structure of the cylindrical wiggler magnetic field in area I (drift chamber) for sequence of iron-aluminum rings

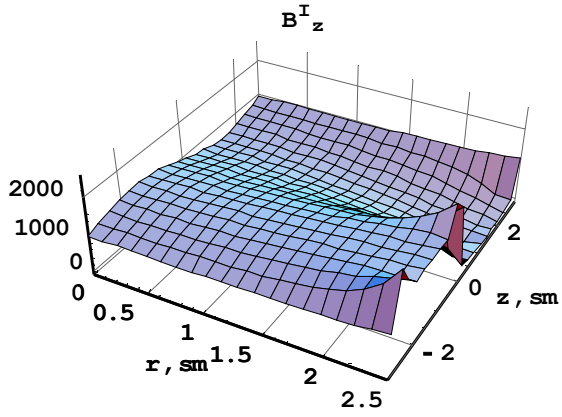

ВОПРОСЫ АТОМНОЙ НАУКИ И ТЕХНИКИ. 2004. № 4.
Серия: Плазменная электроника и новые методы ускорения (4), с. 118-123.

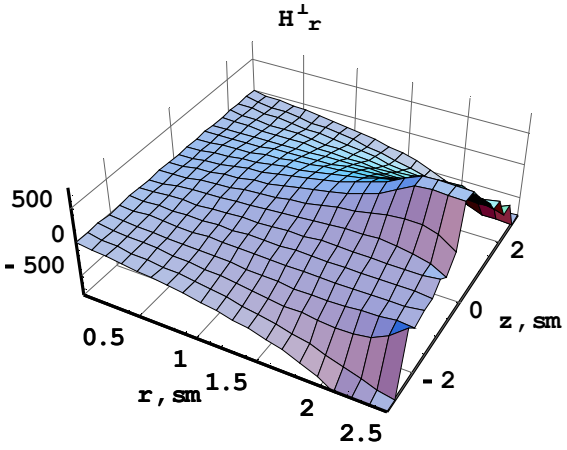

Fig.2. The same in Fig.1 for sequence of iron rings with vacuum gaps

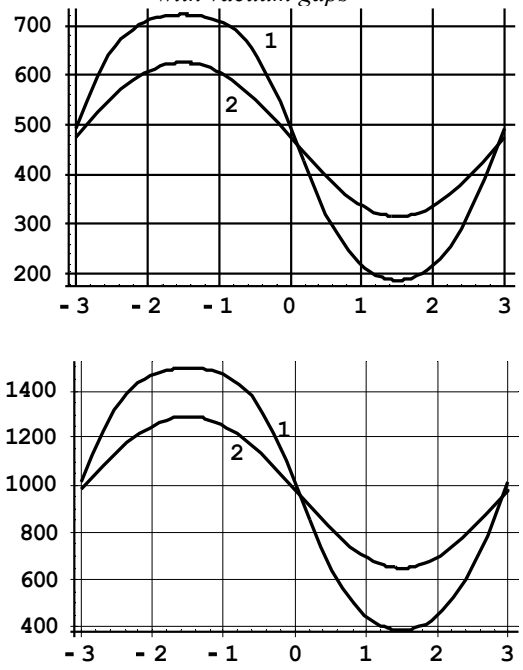

Fig.3. Axial component of the magnetic induction on the axis of our system r=0 (1) and on beam surface $r=r_b=1,6$ cm (2) for one structure period for sequence of iron-aluminum rings (upper picture) and for sequence of iron rings with vacuum gaps (lower picture)

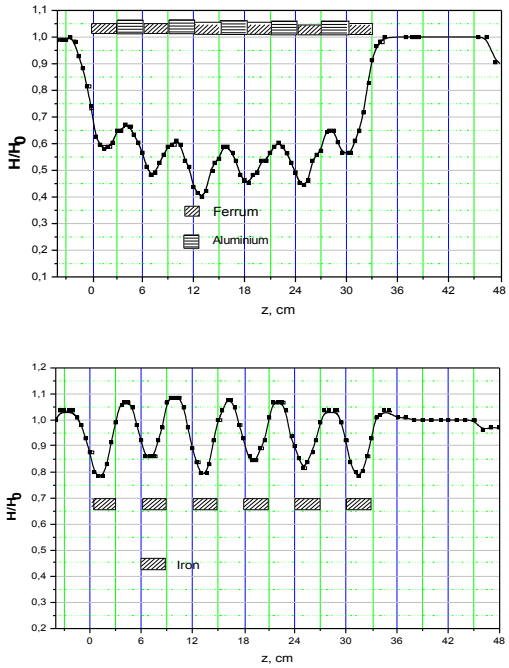

Fig.4. Axial component of the magnetic induction vector on the axis of experimental installation "Agate" in case of iron-aluminum rings (upper picture) and in case of iron rings with vacuum gaps (lower picture)

In Fig.4 the experimentally measured longitudinal distributions of axial component of the magnetic induction in drift chamber of experimental installation "Agate" in case of iron-aluminum rings and in case of iron rings with vacuum gaps. Measurings were carried out with the help of magnetic probes in diameter 30 mm. The average values of the magnetic induction are in well agreement with experimental results for both cases.

We have carried out calculations for dependence of average values of the magnetic induction and for modulation depth on spatial and time period, rings thickness and width. The results of calculations are shown in Fig.5-10.

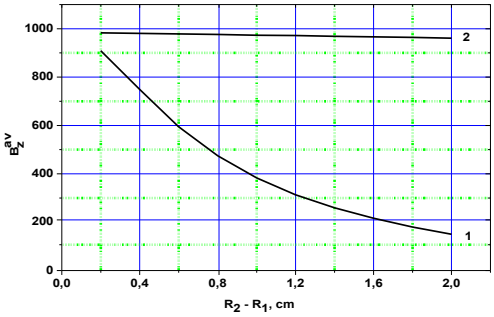

Fig.5. Average value axial component of the magnetic induction versus rings thickness (R_1 = 2.5cm) for the sequence of iron-aluminum rings (1) and for sequence of iron rings with vacuum gaps (2)

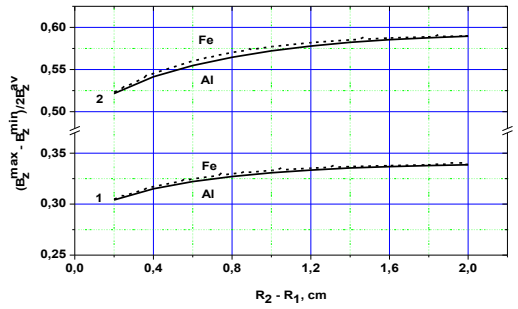

Fig.6. Modulation depth of the magnetic induction versus rings thickness ($R_1 = 2.5cm$) at the structure axis $r = 0$ (1) and at the beam surface $r = r_b$ (2) for sequence of iron-aluminum rings (solid lines) and for sequence of iron rings with vacuum gaps (dashed lines)

In order to understand better the results of a numerical analysis we shall find expression for longitudinal component of magnetic induction in impedance approximation. For this purpose we shall set on boundary of the drift channel a field B_z^I as

$$B_z^I = \begin{cases} B_z^A, & -L/2 \le z \le 0, \\ B_z^B, & 0 \le z \le L/2. \end{cases}$$

As well as above we shall look for the longitudinal magnetic field in form . If not to take into account wave processes $(\omega/c, k_3) << k_n$ $(k_n = 2\pi n/L)$ for distribution B_z^I we shall obtain the following expression

$$B_z^I = \frac{B_z^A + B_z^B}{2}\left(1 - \frac{4}{\pi}\frac{B_z^A - B_z^B}{B_z^A + B_z^B}\sum_{n=0}^{n=\infty}\frac{I_0(k_{2n+1}r)}{I_0(k_{2n+1}R_1)}\frac{\sin(k_{2n+1}z)}{2n+1}\right).$$

As follows from expression the average value of magnetic induction inside drift chamber

$$B_z^{av} = (B_z^A + B_z^B)/2$$

depends from values of magnetic induction on inner surfaces of one and other ring. Whereas the modulation of magnetic induction

$$\alpha = \frac{4}{\pi}\frac{B_z^A - B_z^B}{B_z^A + B_z^B}\sum_{n=0}^{n=\infty}\frac{I_0(k_{2n+1}r)}{I_0(k_{2n+1}R_1)(2n+1)}\cdot\frac{B_z^{\max} - B_z^{\min}}{2B_z^{av}}$$

depends in an explicit form from structure period and

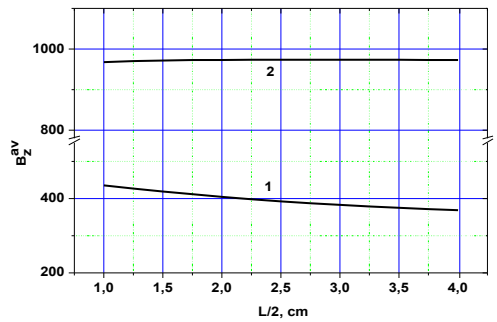

Fig.7. Average value axial component of the magnetic induction versus rings width for the sequence of iron-aluminum rings (1) and for sequence of iron rings with vacuum gaps (2)

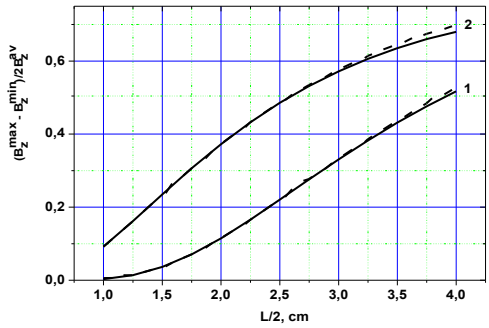

Fig.8. Modulation depth of the magnetic induction versus rings width the structure axis $r = 0$ (1) and at the beam surface $r = r_b$ (2) for the sequence of iron-aluminum rings (solid lines) and for sequence of iron rings with vacuum gaps (dashed lines)

from values of magnetic induction on inner surfaces of one and other rings. In comparisons results of numerical calculations with analytic expressions , we keep in mind that values B_z^A and B_z^B depend from ring sizes, permeability and permittivity of ring materials by implicit way. Let for the sake of definiteness that B_z^A corresponds to nonmagnetic material and B_z^B corresponds to magnetic material. At thickness of iron rings there is vastly greater than a skin layer depth in iron ring $(R_2 - R_1) >> c/\sqrt{2\pi\sigma_2\mu_2\omega}$ it is possible to count approximately $B_z^B \approx 0$. Then

$$B_z^{av} = B_z^A/2, \quad \alpha = \frac{4}{\pi}\sum_{n=0}^{n=\infty}\frac{I_0(k_{2n+1}r)}{I_0(k_{2n+1}R_1)(2n+1)}.$$

That is average value of magnetic induction is dictated by value of magnetic induction on inner surfaces of ring of nonmagnetic material only. The modulation value depends from ring width (structure period L) only.

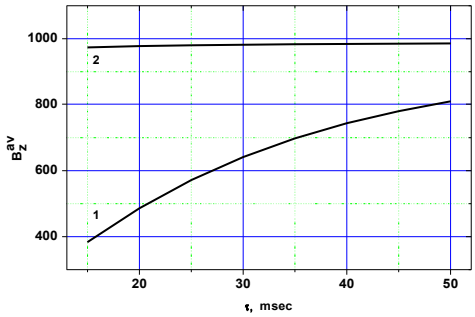

Fig.9. Average value axial component of the magnetic induction versus time period for the sequence of iron-aluminum rings (1) and for sequence of iron rings with vacuum gaps (2)

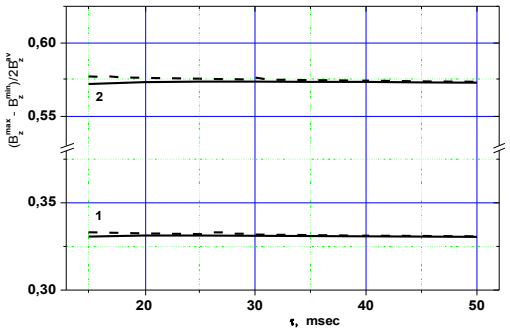

Fig.10. Modulation depth of the magnetic induction versus rings width the structure axis $r = 0$ (1) and at the beam surface $r = r_b$ (2) for the sequence of iron-aluminum rings (solid lines) and for sequence of iron rings with vacuum gaps (dashed lines)

As follows from Fig.5, Fig.7 and Fig.9 average value of longitudinal component of magnetic induction has very weak dependence from on rings thickness, ring width and time period for sequence of iron rings with vacuum gaps and approximately equals to external magnetic field induction. In contrast to this case average value of longitudinal component of magnetic induction for sequence of iron-aluminum rings is strongly decreases when increasing of rings thickness and when increasing of a frequency of external magnetic field changing. Such behavior easily speaks from expression (16) and given there explanations. In case for sequence of iron rings with vacuum gaps the magnetic induction does not decay ($\sigma_2 = 0$) through cross section of gaps, and so it doesn't depend from structure parameters. Because of presence iron rings the value of magnetic induction on inner surfaces of iron ring approximately twice there is more than induction of an exterior magnetic field. The behavior average value of of magnetic induction in case of iron-aluminum ring sequence also it is possible to explain from change of skin depth in aluminum rings.

Fig.6, Fig.8 and Fig.10 show modulation depth independence from rings material. The modulation value depends mainly from structure period.

V. SUMMARIES

1.The set of equations describing the magnetic field of the solenoid with rings made from materials with different electric and magnetic properties is obtained. The current in solenoid varies under the monochromatic law, generally, with the arbitrary frequency.

2.At the low-frequency, period of the structure and rings thickness exerts the essential influence on the magnitude of the magnetic field modulation in contrast to materials of the rings and time period. Modulation depth grows with the axial period increase, and with the rings thickness increase.

3.For parameters of the collective ion accelerator [7] the magnitude of longitudinal magnetic field modulation on the axis of the drift chamber is about 33%, and on the beam radius is about 56%.

The work is carried out with the partial support of the STCU grant #1569.

REFERENCES

1. J.B. Fainberg, N.A. Khizhnyak // *Zh. Tekh. Fiz*. 1955, 25, 711 (in Russian).
2. N.A. Khizhnyak // *RiE. Radioélektron*. 1960, 3, 413 (in Russian).
3. S.I. Molokovskij, A.D. Suhkov. Intensive electron and ion beams. M. Energoatomizdat, 1991 (in Russian).
4. R.H. Jackson, H.P. Freund, D.E. Pershing, J.M. Taccetti // *Nucl. Instr. and Meth. in Phys. Res*. 1994, A341, 454.
5. A.G. Lymar, N.A. Khizhnjak, B.B. Belikov // *VANT. Series: High-energy physics and atomic nucleus*. 1973, 3(5), 78 (in Russian).
6. Yu.V. Tkach, Ya.B. Fainberg, N.P. Gadetskij, et al. // *Pis'ma Zh. Éhksp. Teor. Fiz*. 1975, 22, 136 (in Russian).
7. V.A. Balakirev, A.M. Gorban, I.I. Magda, et al. // *Fizika Plazmy*. 1997, 23, 350 (in Russian).

ФОРМИРОВАНИЕ ПЕРИОДИЧЕСКИХ МАГНИТНЫХ ПОЛЕЙ ПОСЛЕДОВАТЕЛЬНОСТЬЮ КОЛЕЦ С РАЗЛИЧНЫМИ ЭЛЕКТРИЧЕСКИМИ И МАГНИТНЫМИ СВОЙСТВАМИ

Д.Ю. Копейченко, И.Н. Онищенко, Г.В. Сотников, С.С. Пушкарев, Ю.В. Прокопенко, П.Т. Чупиков, Д.В. Медведев

Проведен электродинамический расчет топографии постоянных магнитных полей, создаваемых в пространственно-периодической системе, представляющей собой соленоид, внутри которого периодически размещаются кольца из материалов с различными электрическими и магнитными свойствами.

ФОРМУВАННЯ ПЕРІОДИЧНИХ МАГНІТНИХ ПОЛІВ ПОСЛІДОВНІСТЮ КІЛЕЦЬ З РІЗНИМИ ЕЛЕКТРИЧНИМИ ТА МАГНІТНИМИ ВЛАСТИВОСТЯМИ

Д.Ю. Копійченко, І.М. Онищенко, Г.В. Сотніков, С.С. Пушкарьов, Ю.В. Прокопенко, П.Т. Чупиков, Д.В. Медведев

У роботі проведено електродинамічний розрахунок топографії постійних магнітних полів, що виникають у просторово-періодичній системі, яка являє собою соленоїд, періодично навантажений кільцями з різними електричними та магнітними властивостями.